

Prediction and Power in Molecular Sensors: Uncertainty and Dissipation When Conditionally Markovian Channels Are Driven by Semi-Markov Environments

Sarah E. Marzen^{1,*} and James P. Crutchfield^{2,†}

¹*Physics of Living Systems, Department of Physics,
Massachusetts Institute of Technology, Cambridge, MA 02139*

²*Complexity Sciences Center and Department of Physics,
University of California at Davis, One Shields Avenue, Davis, CA 95616*

(Dated: November 2, 2021)

Sensors often serve at least two purposes: predicting their input and minimizing dissipated heat. However, determining whether or not a particular sensor is evolved or designed to be accurate and efficient is difficult. This arises partly from the functional constraints being at cross purposes and partly since quantifying the predictive performance of even *in silico* sensors can require prohibitively long simulations. To circumvent these difficulties, we develop expressions for the predictive accuracy and thermodynamic costs of the broad class of conditionally Markovian sensors subject to unifilar hidden semi-Markov (memoryful) environmental inputs. Predictive metrics include the instantaneous memory and the mutual information between present sensor state and input future, while dissipative metrics include power consumption and the nonpredictive information rate. Success in deriving these formulae relies heavily on identifying the environment’s causal states, the input’s minimal sufficient statistics for prediction. Using these formulae, we study the simplest nontrivial biological sensor model—that of a Hill molecule, characterized by the number of ligands that bind simultaneously, the sensor’s cooperativity. When energetic rewards are proportional to total predictable information, the closest cooperativity that optimizes the total energy budget generally depends on the environment’s past hysteretically. In this way, the sensor gains robustness to environmental fluctuations. Given the simplicity of the Hill molecule, such hysteresis will likely be found in more complex predictive sensors as well. That is, adaptations that only locally optimize biochemical parameters for prediction and dissipation can lead to sensors that “remember” the past environment.

PACS numbers: 02.50.-r 89.70.+c 05.45.Tp 02.50.Ey

Keywords: predictive information rate, information processing, nonequilibrium steady state, thermodynamics

Introduction To perform functional tasks, synthetic nanoscale machines and their macromolecular cousins simultaneously manipulate energy, information, and matter. They are *information engines*—systems that operate by synergistically balancing the energetics of their physical substrate against required information generation, storage, loss, and transformation to support a given functionality. Classically, information engines were conceived as either potential computers [1]—that is, physical systems that can compute anything given the right program—or as Maxwellian-like demons that use information as a resource to convert disordered energy to useful work [2–5]. Recently, investigations into functional computation [6] embedded in physical systems led to studies of the thermodynamics of various kinds of information processing [7], including the thermodynamic costs of information creation [8], noise suppression [9], error correction and synchronization [10], prediction [11–

13], homeostasis [14], learning [15], structure [16], and intelligent control [17].

Due to its broad importance to the survival of biological organisms, here we focus on a specific functional computation in information engines: how sensory subsystems predict their environment. And, we introduce a thermodynamic analysis that can address environmental processes more complex than the memoryless and finite-state Markov sources and Gaussian processes considered in the above cited works.

Evolved and designed sensory systems are often tasked with at least two, potentially competing, objectives: accurately predicting inputs [18, 19] and minimizing required power and heat dissipation [20, 21] [22]. Accurate and energy-efficient predictive models can be used to optimize action policies, for example, to reap increased rewards from the environment, even regardless of one’s particular “reward function” [23–26].

Extracting such models from actual biological sensors requires a nontrivial matching of sensory statistics and sensor structure [14, 27]. Undaunted, much effort has been invested to find minimally dissipative and maxi-

* semarzen@mit.edu

† chaos@ucdavis.edu

mally predictive sensors, often simplifying the challenges by ignoring action policies—how the sensed information is used. Some seek sensor models that maximize a combination of predictive power and (energetic) efficiency; e.g. as in Refs. [12, 27]. Others validate learning rules based on whether or not they maximize the aforementioned objective function [28, 29]. Finally, others compare real biological sensors to *in silico* null models; e.g. as in Ref. [19].

These efforts require calculating predictive and dissipative metrics of sensory models. For realistic null models, estimating predictive power from simulation can require prohibitively long simulations. To circumvent these and related difficulties, then, one desires closed-form expressions for various predictive and dissipative metrics in terms of the generators of environment behavior and of the sensor-channel properties—the input-dependent stochastic dynamical system describing the sensor. The following provides these expressions for quite general sensors: conditionally Markovian channels subject to complex nonequilibrium steady-state environments that are unifilar hidden semi-Markov processes. Our derivations rely heavily on a recent characterization of the minimal sufficient statistics for predicting such complex environments [30].

To illustrate the insights that arise from this, we study an “optimal” Hill molecule model of ligand-gated channels; see Fig. 1. A Hill molecule is a conditionally Markovian channel with its ligand concentration as input. We assume that the ligand concentration is a realization of a semi-Markov process, a generalization over previous efforts that assumed Markovian [12] or Gaussian [27] processes. Our generalization to arbitrarily temporally correlated inputs is necessary when, for instance, the Hill molecule represents a nicotinic acetylcholine receptor on a synapse and ligands are acetylcholine molecules since, as a practical matter, neuronal dynamics are often non-Markovian and non-Gaussian [31]. As a result, we find that (i) increases in cooperativity (memory) of the Hill molecule lead to increases in both predictive power and power consumption, (ii) a large fraction of power consumption comes from inefficient prediction, and (iii) simple gradient-based adaptation rules lead to hysteresis.

Background Central to our analysis is an appreciation of causal states (minimal sufficient statistics of prediction and/or retrodiction), unifilar hidden semi-Markov processes, and conditionally Markovian channels. We review these concepts here, simultaneously introducing relevant notation.

Environment Input symbols x take on any value in the observation alphabet \mathcal{A} . We code the *past* of the input time series as $\overleftarrow{x} = \dots(x_{-2}, \tau_{-2}), (x_{-1}, \tau_{-1}), (x_0, \tau_+)$ and the in-

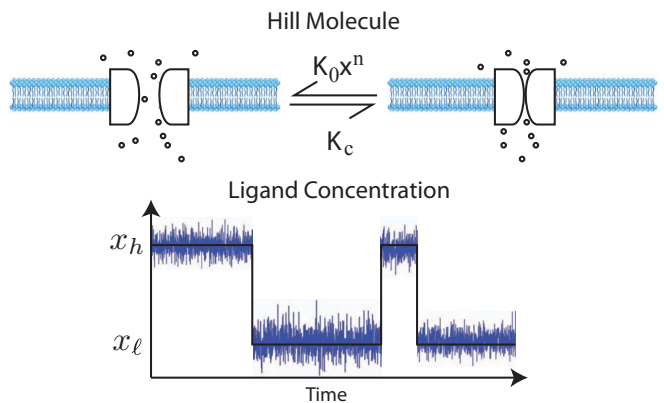


FIG. 1. Hill molecule: (Top) Ion channel in a neuronal membrane in the open (left) and closed (right) states in which ions can and cannot travel through. (Below) Ligand concentrations during the open-closed cycle of the molecule.

put’s *future* as $\overrightarrow{x} = (x_0, \tau_-), (x_1, \tau_1), (x_2, \tau_2), \dots$, where τ_i is the total dwell time for symbol x_i . To ensure a unique coding, we stipulate that $x_i \neq x_{i+1}$. Note that symbol x_0 is seen for a total dwell time of $\tau_+ + \tau_- = \tau_0$; that is, the present splits the dwell time τ_0 into two.

As is typical, \overleftarrow{X} is the random variable corresponding to semi-infinite input pasts and \overrightarrow{X} the random variable corresponding to semi-infinite input futures. We now briefly review the definition of causal states, as described in Ref. [32]. Forward-time causal states \mathcal{S}^+ , the minimal sufficient statistics for prediction, are defined via the following equivalence relation: two semi-infinite pasts, \overleftarrow{x} and \overleftarrow{x}' , are considered “predictively” equivalent if:

$$\overleftarrow{x} \sim_{\epsilon^+} \overleftarrow{x}' \Leftrightarrow \Pr(\overrightarrow{X} | \overleftarrow{X} = \overleftarrow{x}) = \Pr(\overrightarrow{X} | \overleftarrow{X} = \overleftarrow{x}').$$

The relation partitions the set of semi-infinite pasts into clusters of pasts. Each cluster is a *forward-time causal state* σ^+ . *Reverse-time causal states* \mathcal{S}^- , the minimal sufficient statistics for retrodiction, are defined similarly. Two semi-infinite futures, \overrightarrow{x} and \overrightarrow{x}' , are considered “retrodictively” equivalent if:

$$\overrightarrow{x} \sim_{\epsilon^-} \overrightarrow{x}' \Leftrightarrow \Pr(\overleftarrow{X} | \overrightarrow{X} = \overrightarrow{x}) = \Pr(\overleftarrow{X} | \overrightarrow{X} = \overrightarrow{x}').$$

This equivalence relation partitions the set of semi-infinite futures into clusters, each cluster being a reverse-time causal state σ^- .

Forward- and reverse-time causal states are useful in the ensuing calculations due to the following Markov chains. First, forward-time causal states are a deterministic function of the input past ($\sigma^+ = \epsilon^+(\overleftarrow{x})$), and reverse-time causal states are a deterministic function of the input future ($\sigma^- = \epsilon^-(\overrightarrow{x})$). Hence, we have the Markov chains $\mathcal{S}^+ \rightarrow \overleftarrow{X} \rightarrow \overrightarrow{X}$ and $\mathcal{S}^- \rightarrow \overleftarrow{X} \rightarrow \overrightarrow{X}$.

However, causal states are minimal sufficient statistics of the past relative to the future and vice versa. And so, $\overleftarrow{X} \rightarrow \mathcal{S}^+ \rightarrow \overrightarrow{X}$ and $\overrightarrow{X} \rightarrow \mathcal{S}^- \rightarrow \overleftarrow{X}$ are also valid Markov chains. Invoking these Markov chains is called *causal shielding*.

Let's first address the more general case of unifilar hidden semi-Markov input, as in Ref. [30]. Forward-time hidden states are labeled g , and causal states are thus labeled by (g, x_+, τ_+) . That is, the forward-time hidden state g , current emitted symbol x_+ , and time since last symbol τ_+ together comprise the forward-time causal states for unifilar hidden semi-Markov input processes. Dwell times are drawn from $\phi_g(\tau)$; emitted symbols are chosen with probability $p(x|g)$; and $g = \epsilon^+(g', x')$ is the next hidden state given that the current hidden state is g' and the current emitted symbol is x' .

For the Hill molecule, we focus on semi-Markov input. This greatly constrains the forward- and reverse-time causal states, so that g and x_+ are equivalent. The forward-time causal states are thus described by the pair (x_+, τ_+) , where x_+ is the input symbol infinitesimally prior to the present and τ_+ is the time since last symbol (i.e., x_{-1}). The reverse-time causal states are similarly described by the pair (x_-, τ_-) , where x_- is the input symbol infinitesimally after the present and τ_- is the time to next symbol (i.e., x_1). Let \mathcal{T}_\pm be the random variable describing time since (to) last (next) symbol. The dwell time of symbol x has probability density function $\phi_x(\tau)$, and the probability of observing symbol x after x' is $q(x|x')$. By virtue of how we have chosen to encode our input: $q(x|x) = 0$.

Finally, the development to come requires our finding the joint distribution $\rho(\sigma^+, \sigma^-)$ of forward- and reverse-time causal states. When the input is unifilar hidden semi-Markov, efficiently finding $\rho(\sigma^+, \sigma^-)$ is an open problem. Nonetheless, we can say:

$$\begin{aligned} \rho(\sigma^- | \sigma^+) &= \rho(g_-, x_-, \tau_- | g_+, x_+, \tau_+) \\ &= \delta_{x_+, x_-} \frac{\phi_{g_+}(\tau_+ + \tau_-)}{\Phi_{g_+}(\tau_+)} p(g_+ | g_-, x_-) . \end{aligned}$$

For semi-Markov input, this simplifies: $\rho(\sigma^+, \sigma^-) = \rho((x_+, \tau_+), (x_-, \tau_-))$. As described in Ref. [30], we have:

$$\rho(x_+, \tau_+) = \mu_{x_+} \Phi_{x_+}(\tau_+) p(x_+) \quad (1)$$

where:

$$\Phi_{x_+}(\tau_+) = \int_{\tau_+}^{\infty} \phi_{x_+}(t) dt, \quad \mu_{x_+} = 1 / \int_0^{\infty} t \phi_{x_+}(t) dt ,$$

and $p(x_+)$ is the probability of observing symbol x_+ .

The latter probability is given by:

$$p(x_+) = (\text{diag}(1/\mu_x) \text{eig}_1(q))_{x_+} .$$

The conditional distribution of reverse-time causal states given forward-time causal states is then:

$$\begin{aligned} \rho(\sigma^- | \sigma^+) &= \rho((x_-, \tau_-) | (x_+, \tau_+)) \\ &= \frac{\phi_{x_+}(\tau_+ + \tau_-)}{\Phi_{x_+}(\tau_+)} \delta_{x_+, x_-} . \end{aligned} \quad (2)$$

Together, Eqs. (1) and (2) give the joint distribution $\rho(\sigma^+, \sigma^-) = \rho(\sigma^+) \rho(\sigma^- | \sigma^+)$.

Sensory channel We assume the channel is conditionally Markovian. As such, its dynamics are fully specified by input state-dependent kinetic rates. More precisely, the channel state y , with corresponding random variable Y , can take on any value in \mathcal{Y} , and the rate at which channel state y transfers to channel state y' when the input has value x is given by:

$$k_{y \rightarrow y'}(x) := - \sum_{y''} k_{y \rightarrow y''}(x) .$$

Then, the probability $p(y, t)$ of being in channel state y at time t evolves as:

$$\frac{dp(y, t)}{dt} = \sum_{y'} k_{y' \rightarrow y}(x(t)) p(y', t) ,$$

where $x(t)$ is the input symbol at time t .

To simplify notation and ease computation, we write dynamical evolution rules in matrix-vector form. Let $\vec{p}(y, t)$ be the vector of probabilities that the channel is in a particular state y at time t , and let $M(x)$ be a matrix of rates: $M_{y', y}(x) = k_{y' \rightarrow y}(x)$. Then, we have:

$$\frac{d\vec{p}(y, t)}{dt} = M(x(t)) \vec{p}(y, t) . \quad (3)$$

With this, it is clear that $\vec{p}(y, t)$ can oscillate or decay to a steady state. The Perron-Frobenius theorem guarantees that:

$$p_{eq}(x) := \text{eig}_0(M(x)) ,$$

the probability distribution over channel states when ligand concentration is set to x , is unique.

Sensor Accuracy and Thermodynamics We now introduce and justify predictive and dissipative metrics, present closed-form expressions for these metrics in terms of aforementioned generators and channels, and explore the relationship between cooperativity in biochemical sensing and prediction and dissipation.

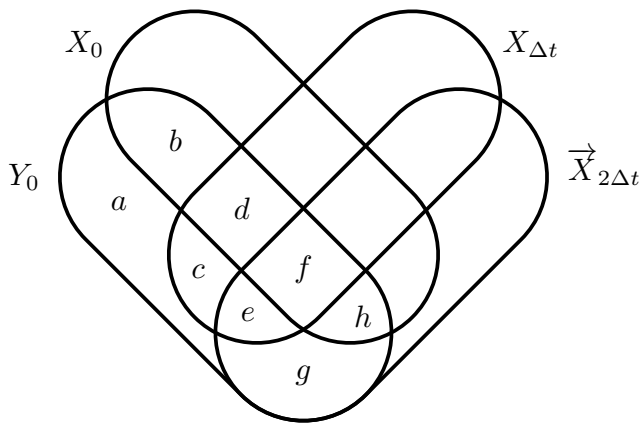


FIG. 2. Sensor information diagram [33] giving the relationship between predictive metrics and nonpredictive information rate. Instantaneous memory is $I_{\text{mem}} = I[X_0; Y_0] = b + d + f + h$ and total predictable information $I_{\text{fut}} = \lim_{\Delta t \rightarrow 0} I[Y_0; X_0] = \lim_{\Delta t \rightarrow 0} b + c + d + e + f + g + h$, while the lower bound on power consumption, the nonpredictive information rate is $\dot{I}_{\text{np}} = \lim_{\Delta t \rightarrow 0} \frac{b+h-c-e}{\Delta t}$. Recall $a = H[Y_0|X_0, X_{\Delta t}, \vec{X}_{2\Delta t}]$, $b = I[Y_0; X_0|X_{\Delta t}, \vec{X}_{2\Delta t}]$, $f = I[Y_0; X_0; X_{\Delta t}; \vec{X}_{2\Delta t}]$, and so on.

Predictive and dissipative metrics We employ several metrics to quantify the sensor predictive performance and their energy efficiency. *Instantaneous memory* I_{mem} [11] and *total predictable information* I_{fut} [29, 34] characterize predictive power, while the *nonpredictive information rate* \dot{I}_{np} [11–13] and temperature-normalized *power consumption* βP monitor dissipation. Figure 2 uses an information diagram [33, 35] to illustrate their relations in terms of the elementary information atoms—entropies, conditional entropies, and mutual informations—out of which they are constructed.

Our selection of metrics differs from previous efforts to characterize prediction and dissipation. For instance, the instantaneous predictive information in Ref. [11] is equivalent to instantaneous memory to $O(\Delta t)$ in a continuous-time framework. Similarly, Ref. [13] focused on instantaneous memory and nonpredictive information rate, but did not calculate total predictable information or a more standard prediction-related metric. Reference [12] used the ratio of nonpredictive information rate to entropy production to characterize learning, but nonpredictive information rate is not a typical metric for predictive power in machine learning or related literature. Finally, Ref. [27] focused on metrics for prediction, including a natural continuous-time extension of instantaneous predictive information, but not on metrics for dissipation.

There is little consensus on quantifying a channel’s predictive capability. Common metrics are designed to quantify *memory* rather than *prediction* [36], but even

when adapted for measuring prediction, one can choose different types of readout function. We focus on what we call the *total predictable information*:

$$I_{\text{fut}} := I[Y; \vec{X}] .$$

This is the mutual information between present channel state and the input’s future. It is the amount of information that is predictable about the input future from the present channel state. Due to the feedforward nature of the channel-input setup—that is, the channel’s state does not affect the input—and the Markov chains given earlier, we have the Markov chain $Y \rightarrow \mathcal{S}^+ \rightarrow \mathcal{S}^- \rightarrow \vec{X}$. As a result:

$$I_{\text{fut}} = I[Y; \mathcal{S}^-] = I[Y; X_-, \mathcal{T}_-] ,$$

which decomposes into:

$$I_{\text{fut}} = I[Y; X_-] + I[Y; \mathcal{T}_- | X_-] .$$

The term $I[Y; X_-]$ is called the *instantaneous memory* I_{mem} [11], since it is the amount of information available from the channel state about the just-seen input symbol. We find that:

$$I_{\text{fut}} = I_{\text{mem}} + I[Y; \mathcal{T}_- | X] .$$

Thus, the total predictable information is the sum of instantaneous memory and information that is truly about the future, which here is the time to next symbol.

The Supplementary Material justifies I_{fut} on generational timescales as a metric via an extension of Kelly’s classic bet-hedging argument [37]. In a discrete-time setting, increases in growth rate via increases in sensory information is equal to the instantaneous predictable information $I[Y_0; X_{\Delta t}]$. The total predictable information I_{fut} is an upper bound on this increase in growth rate. On ontogenetic timescales, we merely assert that total predictable information might increase concurrently with energetic rewards.

Next, we need to quantify the power consumed by the sensor system. Assuming access to a temperature-normalized “energy function” $\beta E(x, y)$, the temperature-normalized power βP is given by:

$$\beta P = \lim_{\Delta t \rightarrow 0} \frac{\langle \beta E(x_{t+\Delta t}, y_t) \rangle - \langle \beta E(x_t, y_t) \rangle}{\Delta t} . \quad (4)$$

If determining an energy function is not possible, we can calculate a lower bound using a continuous-time adaptation of the inequality in Ref. [11]:

$$\dot{I}_{\text{np}} := \lim_{\Delta t \rightarrow 0} \frac{I[Y_t; X_t] - I[Y_t; X_{t+\Delta t}]}{\Delta t} \leq \beta P , \quad (5)$$

with an alternate equivalent definition in Ref. [13]; see the Supplementary Material.

\dot{I}_{np} is called the *nonpredictive information rate* since it loosely corresponds to how much of the instantaneous memory is useless for predicting the next input. Reference [12] viewed $\dot{I}_{\text{np}}/\beta P$ as a learning efficiency. We take the view that \dot{I}_{np} is a potentially useful lower bound on temperature-normalized power consumption, and use I_{mem} and I_{fut} instead to characterize learning. Any differences between the formulae shown here and Ref. [11, Eq. (2)] are superficial; we merely adapted the derivation for continuous-time processes. Unfortunately, no one has yet given a guarantee that the nonpredictive information rate is a tight lower bound on temperature-normalized power.

Closed-form metrics As stated earlier, we wish to find closed-form expressions for I_{fut} , I_{mem} , \dot{I}_{np} , and βP in terms of input properties— $\phi_x(\tau)$, $\epsilon^+(g, x)$, $p(x|g)$ —and channel properties— $M(x)$. Their derivations are too lengthy for here and so are relegated to the Supplementary Materials (SM). The appropriate equations there are referenced here, where relevant.

Calculating I_{fut} and I_{mem} can be accomplished once $\rho(\sigma^+, y) = \Pr(\mathcal{S}^+ = \sigma^+, Y = y)$ is obtained. This follows, in turn, by manipulating a Chapman-Kolmogorov equation, shown in the SM. Set any ordering on the pairs (g, x) ; e.g., the ordering $(g_1, x_1), (g_1, x_2), \dots, (g_{|G|}, x_{|A|})$. An expression for $p(y|\sigma^+) = p(y|g, x, \tau)$ is given by a combination of Eqs. (S11) and (S15):

$$p(y|g, x, \tau) = \left(e^{M(x)\tau} \text{eig}_1(\mathbf{C})_{(g,x)} / \mu_g p(g) \right)_y,$$

where \mathbf{C} is a block matrix with entries $\mathbf{C}_{(g,x),(g',x')} = \delta_{g,\epsilon^+(g',x')} p(x'|g') \int_0^\infty \phi_{g'}(t) e^{M(x')t} dt$. And so, $\text{eig}_1(\mathbf{C})$ is a block vector. Normalization forces $\bar{\Gamma}^\top \text{eig}_1(\mathbf{C})_{(g,x)} = \mu_g p(g)$.

We then find the joint probability distribution as $\rho(y, \sigma^+) = p(y|\sigma^+) \rho(\sigma^+)$, which enables computation of all predictive metrics. Instantaneous memory is given by $I_{\text{mem}} = \text{I}[X; Y]$, whereas $I_{\text{fut}} = \text{I}[Y; \mathcal{S}^-]$. All the relevant distributions—namely, $p(x, y)$ and $\rho(\sigma^-, y)$ —are obtained from the previously derived $\rho(\sigma^+, y)$. For instance, to calculate $\rho(\sigma^-, y)$, we employ the previously stated Markov chain to find:

$$\rho(\sigma^-, y) = \sum_{\sigma^+} \rho(\sigma^- | \sigma^+) p(y|\sigma^+) \rho(\sigma^+).$$

And, to calculate $p(x, y)$, we recall that $\sigma^- = (x, \tau_-)$, so we only need marginalize the joint distribution of $\rho((x, \tau_-), y)$.

Calculation of dissipative metrics can be additionally

accomplished once:

$$\frac{\delta p(x, y)}{\delta t} = \lim_{\Delta t \rightarrow 0} \left(\Pr(X_{t+\Delta t} = x, Y_t = y) - \Pr(X_t = x, Y_t = y) \right) / \Delta t$$

is obtained. An expression for $\frac{\delta p}{\delta t}$ in terms of input and channel properties is given in Eq. (S17):

$$\begin{aligned} \frac{\delta p}{\delta t} &= \sum_{g', x' \neq x} \int d\tau' p(x|\epsilon^+(g', x')) p(x'|g') \phi_{g'}(\tau') \\ &\times \left(e^{M(x')\tau'} \text{eig}_1(\mathbf{C})_{(g', x')} \right)_y \\ &- \sum_{g'} \int d\tau' p(x|g') \phi_{g'}(\tau') \left(e^{M(x)\tau'} \text{eig}_1(\mathbf{C})_{(g', x)} \right)_y, \end{aligned}$$

where normalization again requires $\bar{\Gamma}^\top \text{eig}_1(\mathbf{C})_{(g,x)} = \mu_x p(g)$. Then, from earlier, we find that:

$$\dot{I}_{\text{np}} = \lim_{\Delta t \rightarrow 0} \frac{H[Y_t, X_{t+\Delta t}] - H[Y_t, X_t]}{\Delta t} \quad (6)$$

$$\begin{aligned} &= \lim_{\Delta t \rightarrow 0} \left(\sum_{x,y} \left(p(x, y) + \frac{\delta p}{\delta t} \Delta t \right) \log \frac{1}{p(x, y) + \frac{\delta p}{\delta t} \Delta t} \right. \\ &\quad \left. - \sum_{x,y} p(x, y) \log \frac{1}{p(x, y)} \right) / \Delta t \quad (7) \end{aligned}$$

$$= - \sum_{x,y} \frac{\delta p(x, y)}{\delta t} \log p(x, y). \quad (8)$$

When there are no nondecaying oscillations in $\vec{p}(y, t)$ [38], we can find βP despite lacking direct access to an energy function by calculating the steady-state distribution over channel states with fixed input:

$$\vec{p}_{\text{eq}}(y|x) = \text{eig}_0(M(x)) = \frac{e^{-\beta E(x,y)}}{Z_\beta(x)},$$

where the partition function is $Z_\beta(x) := \sum_y e^{-\beta E(x,y)}$. Hence:

$$\beta E(x, y) = \log \frac{1}{p_{\text{eq}}(y|x)} - \log Z_\beta(x). \quad (9)$$

Recalling Eq. (4) and invoking stationarity—that $\Pr(X_t = x) = \Pr(X_{t+\Delta t} = x)$ —yields:

$$\begin{aligned} \beta P &= \lim_{\Delta t \rightarrow 0} \left(\left\langle \log \frac{1}{p_{\text{eq}}(x, y)} \right\rangle_{\Pr(X_{t+\Delta t}=x, Y_t=y)} \right. \\ &\quad \left. - \left\langle \log \frac{1}{p_{\text{eq}}(x, y)} \right\rangle_{\Pr(X_t=x, Y_t=y)} \right) / \Delta t \quad (10) \end{aligned}$$

$$= \sum_{x,y} \frac{\delta p(x, y)}{\delta t} \log \frac{1}{p_{\text{eq}}(y|x)}. \quad (11)$$

The distributions $\Pr(X_{t+\Delta t} = x, Y_t = y)$ and $\Pr(X_t = x, Y_t = y)$ can be obtained from $M(x)$. In other words, when there are no recurrent cycles, we can calculate βP directly from the kinetic rates $k_{y \rightarrow y'}(x)$ and input generator $(\phi_g(\tau), \epsilon^+(g, x), p(x|g))$ alone.

Effect of cooperativity on prediction and dissipation

The Hill molecule is a common fixture in theoretical biology, as it is the simplest mechanistic model of cooperativity [39]. Recall Fig. 1. A Hill molecule can be in one of two states, open or closed. When open, n ligand molecules are bound; when closed, no ligand molecules are bound. Hence, the state of the Hill molecule carries information about the number of bound ligand molecules. In other words, such molecules are sensors of their environment.

Let us outline a simple dynamical model of the Hill molecule. The rate of transition from closed C to open O given a ligand concentration x is:

$$k_{C \rightarrow O} = k_O x^n. \quad (12)$$

While the transition rate from open O to closed C is:

$$k_{O \rightarrow C} = k_C. \quad (13)$$

The steady-state distribution given fixed ligand concentration is the familiar:

$$\begin{aligned} \Pr_{\text{eq}}(Y = O | X = x) &= \frac{k_O x^n}{k_C + k_O x^n} \\ &= \frac{x^n}{(k_C/k_O) + x^n}. \end{aligned}$$

Although the mechanistic model makes sense only when n is a nonnegative integer, this model is often used when n is any nonnegative real number; increases in n can still be thought of as increases in cooperativity. Equations (12)-(13) constitute a complete characterization of channel properties.

Increasing the cooperativity n increases the steepness of the molecule's "binding curve"—the probability of being "on" as a function of concentration. In other words, the sensor becomes more switch-like and less a proportionately responding transducer of the input. If the concentration is greater than $(k_C/k_O)^{1/n}$, the switch is essentially "on" if n is high. A more switch-like sensor is useful if the optimal phenotype depends only upon the condition "ligand concentration greater than X". Whereas, a less switch-like, smoother responding sensor helps if the optimal phenotype depends on ligand concentration in a more graded manner.

The concentration scale is set by $(k_C/k_O)^{1/n}$, while the time scale is set by $1/k_C$; as such, we set both to $k_O = k_C = 1$ without loss of generality. We imagine

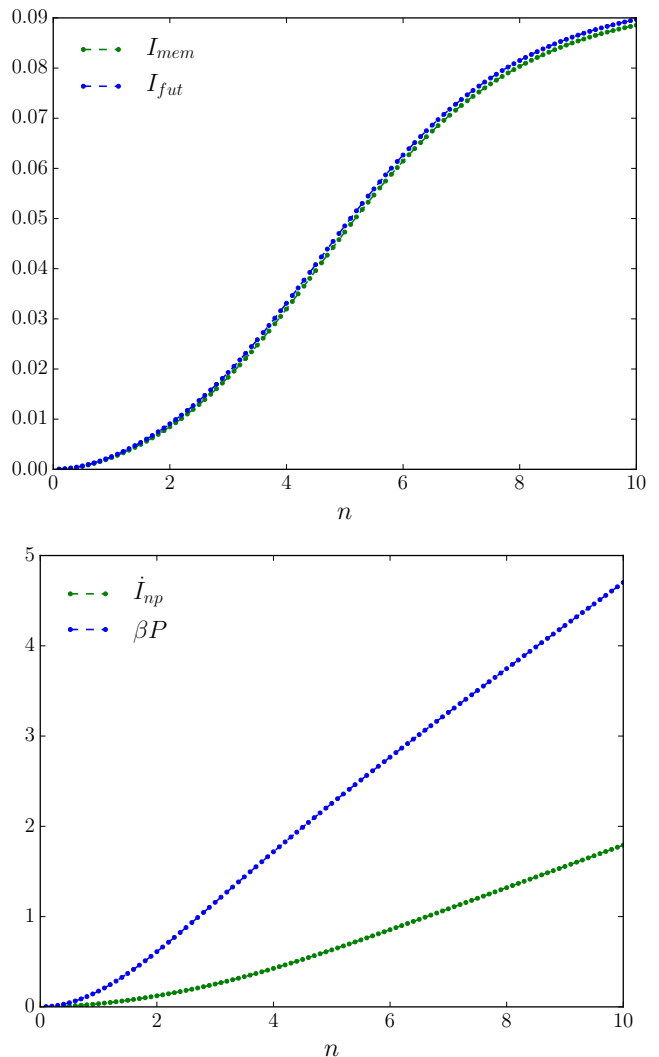


FIG. 3. (Top) Ligand concentration can take one of two values, $x_l = 0.5$ and $x_h = 2.0$, in units of $(k_C/k_O)^{1/n}$. Dwell-time distributions are parametrized as $\phi_x(t) = \lambda(x)^2 t e^{-\lambda(x)t}$ with $\lambda(x_l) = 5$, $\lambda(x_h) = 4$ in units of $1/k_C$. Hill molecule parameters are set to $k_O = k_C = 1$, with varying cooperativity n . (Bottom) prediction-related metrics: instantaneous memory I_{mem} and total predictive power I_{fut} , as functions of n in nats. At right, temperature-normalized dissipation-related metrics: non-predictive information rate \dot{I}_{np} and temperature-normalized power βP , both in nats per unit time.

that the ligand concentration alternates between two values: x_l and x_h . When there is less ligand (x_l), we will tend to see the Hill molecule revert to and stay in the closed state. When there is ligand ($x_h > x_l$), we will tend to see the Hill molecule revert to and stay in the open state. With no particular application in mind, we imagine that the dwell-time distributions take the form $\phi_x(\tau) = \lambda(x)^2 \tau e^{-\lambda(x)\tau}$ with $\lambda(x_l) = 5$ and $\lambda(x_h) = 4$.

We now deploy the earlier formulae to study the pre-

dictive capabilities and dissipative tendencies of a Hill molecule subject to semi-Markov input. Previous studies of biological sensors found that increases in cooperativity accompanied increases in channel capacity [40–42]. Others studied the thermodynamics of prediction of cooperative biological sensors [12, 27], but did not use the more general class of semi-Markov input and did not calculate the full suite of metrics here, leaving much sensor operation untouched.

An example— $x_l = 0.5$, $x_h = 2.0$ and $k_O = k_C = 1.0$, $n = 2$ —illustrates that roughly 99% of I_{fut} is devoted to instantaneous memory I_{mem} and roughly 25% of βP is devoted to \dot{I}_{np} . That is, the inefficiency in choosing what information to store about the present input contributes greatly to energetic inefficiency. These results hold qualitatively even when the dwell-time distributions are log-normal, i.e., are heavier-tailed.

Fig. 3 shows that increased cooperativity—that is, increases in n —lead to increases in predictive performance, qualitatively in line with Ref. [42]. Additionally, the larger the cooperativity, the higher the fraction of I_{mem}/I_{fut} . Larger cooperativity, however, leads to roughly linear increases in the power consumption and the nonpredictive information rate, whereas increases in predictive power take a more sigmoidal shape. We therefore might prefer intermediate values of cooperativity (e.g., $n \approx 5$) to larger values of cooperativity (e.g., $n \geq 10$). This is qualitatively similar to the results of Refs. [40, 41], in that physical constraints can force optimal information transmission at intermediate levels of cooperativity.

In the absence of a reward function, we assert that energetic rewards are proportional to I_{fut} [43, 44], so that the total energy budget is $\alpha I_{fut} - \beta P$. The proportionality constant α is set by the type of environment in which one finds oneself. Then, the total energy budget $\alpha I_{fut} - \beta P$ is optimized by the cooperativity $\hat{n} = \arg \max_n (\alpha I_{fut} - \beta P)$. As both I_{fut} and βP increase monotonically with n , there is generically only one such cooperativity \hat{n} . At lower α , though, there are two local maxima of the function of n given by $\alpha I_{fut} - \beta P$, as shown at Fig. 4(Top). Let’s pursue the consequences of this regime dependence.

There are rules for how sensor biochemical parameters adapt to the present environment. If adaptation rules for cooperativity of a Hill molecule increase the total energy budget by gradient descent then, for a range of α , we expect that the cooperativity of the Hill molecule to be in either of the two local maxima of $\alpha I_{fut} - \beta P$ just noted. We assume a separation of timescales—namely, that cooperativity adapts much more slowly than the longest environmental timescale. Figure 4(Bottom) shows the optimal cooperativity \hat{n} as a function of conversion factor

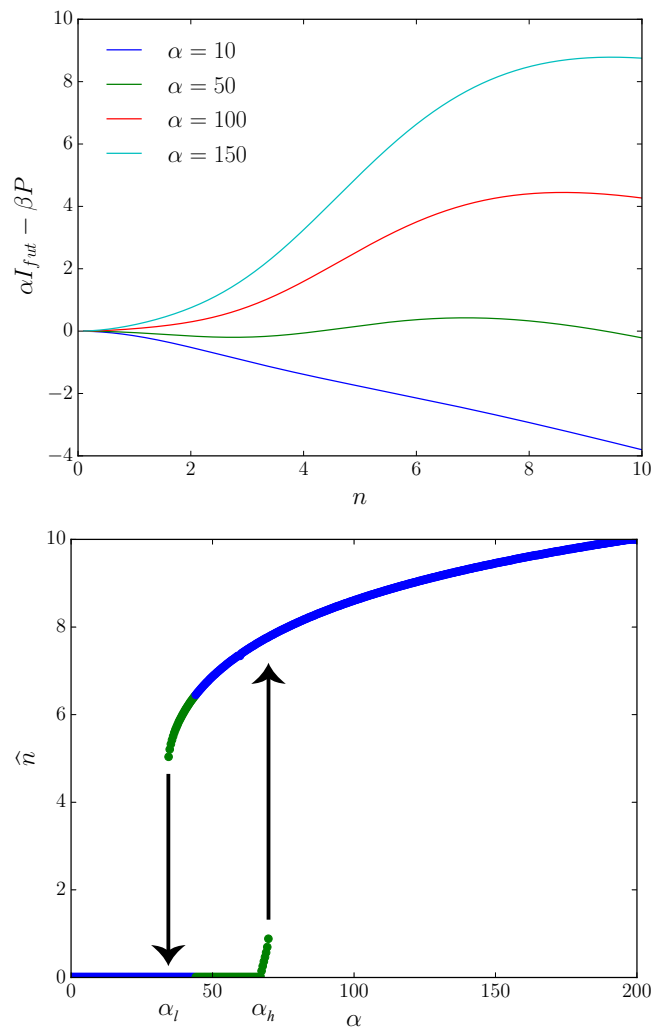


FIG. 4. (Top) “Lagrangian” $\alpha I_{fut} + \beta P$ for several arbitrary α —that represent the energy rewards of I_{fut} —as a function of n . Notice that a particular α singles out a particular optimal \hat{n} . (Bottom) Optimal cooperativity \hat{n} as a function of conversion factor α . Circles (solid blue) are the values of the global maximum \hat{n} and circles (solid green) are local maxima. Arrows indicate the directionality in the hysteresis loop: \hat{n} jumps up at the upper value α_h , if starting at low α , and jumps down at the lower value α_l , if starting at high α .

α . As expected from the presence of two local maxima at lower α , there is a discontinuity (supercritical bifurcation [45]) in the function of α given by $\arg \max_n \alpha I_{fut} - \beta P$. Thus, initially, if α (energetic reward for prediction) increases, the cooperativity discontinuously jumps to a higher \hat{n} at a critical α_h . From there, if one decreases α , optimal cooperativity slowly decreases, but stays high well below α_h , suddenly decreasing to zero cooperativity at the lower value α_l . Thus, there is a substantial hysteresis loop built into the optimal trade-off between energy and sensitivity.

Recall that in switching circuits hysteresis is essen-

tial to adding stability to a switch’s response. Hysteresis stops “race” conditions in which the switch oscillates wildly just as the threshold is passed, amplifying any noise in the control and internal dynamics. In the Hill molecule, hysteresis is helpful if a memory of past environmental conditions (α) provides insight into future conditions (future α). For example, the environment might shift α suddenly to being low, but there is a replenishment mechanism for the available energy that will soon increase α again. Thus, we see that robustness to environmental noise emerges naturally as the sensor adapts to and anticipates changing external conditions.

Conclusion We provided closed-form expressions for instantaneous memory, total predictable information, nonpredictive information rate, and power consumption for a conditionally Markovian channel subject to unifilar hidden semi-Markov input.

In motivating these metrics for prediction and dissipation on general timescales, we appealed to an extension of Kelly’s classic bet-hedging that arises from his information-theoretic analysis of trading-off the benefits of risky, but highly profitable resource investment against the costs of sudden loss [37, 46]. Here, a sensor faces an analogous challenge of high sensitivity but at an energy cost that might be suddenly wasted when the environmental conditions fluctuate. Similar bet-hedging strategies have been implicated in other biological systems, such as in seed germination in annual plants [47] and bacteriophages [48] and in population biology [49, 50] and evolution [46, 51] more generally. The present setting, though, implicates such strategy optimization in a substantially more elementary and primitive biological subsystem.

Finally, we used these formulae to calculate the predictive performance and energetic inefficiency of a simple model of a biological sensor—a Hill molecule. We found that increases in cooperativity yield increases in both predictive performance and energy consumption and that the relative balance between those increases naturally leads to sensor robustness to environmental fluc-

tuations supported by dynamical hysteresis. Given the Hill molecule’s simplicity as a model sensor, we expect to find hysteresis and the resulting robustness in more complex biological sensory systems.

The ease with which these various metrics were calculated masks the difficulty of obtaining the necessary closed-form expressions. (Cf. Supplementary Materials.) We provided universal estimators for various predictive and dissipative metrics for conditionally Markovian channels, as unifilar hidden semi-Markov processes are that general. One practical consequence is that those wishing to study the relationship between prediction and dissipation need not simulate arbitrarily long trajectories. Instead, they can validate or invalidate predictive learning rules and sensor designs using the universal estimators of these predictive and dissipative metrics. Then they can efficiently search through parameter space for “optimal” (predictive and energy-efficient) sensors. In addition, given that the theories of random dynamical systems and of input-dependent dynamical systems are still under development [52], we believe the formulae presented here will lead in those domains to a precise generalization of time-scale matching for nonlinear systems [27].

ACKNOWLEDGMENTS

We thank N. Ay, A. Bell, W. Bialek, S. Dedeo, C. Hillar, I. Nemenman, and S. Still for useful conversations and the Santa Fe Institute for its hospitality during visits, where JPC is an External Faculty member. This material is based upon work supported by, or in part by, the John Templeton Foundation grant 52095, the Foundational Questions Institute grant FQXi-RFP-1609, the U. S. Army Research Laboratory and the U. S. Army Research Office under contract W911NF-13-1-0390. S.E.M. was funded by an MIT Physics of Living Systems Fellowship.

-
- [1] C. H. Bennett. The thermodynamics of computation: a review. *Intl. J. Theo. Physics*, 21(12):905–940, 1982.
 - [2] J. C. Maxwell. *Theory of Heat*. Longmans, Green and Co., London, United Kingdom, ninth edition, 1888.
 - [3] L. Szilard. On the decrease of entropy in a thermodynamic system by the intervention of intelligent beings. *Z. Phys.*, 53:840–856, 1929.
 - [4] D. Mandal and C. Jarzynski. Work and information processing in a solvable model of Maxwell’s demon. *Proc. Natl. Acad. Sci. USA*, 109(29):11641–11645, 2012.
 - [5] S. Deffner and C. Jarzynski. Information processing and the second law of thermodynamics: An inclusive, hamiltonian approach. *Phys. Rev. X*, 3(4):041003, 2013.
 - [6] Here, when analyzing sensory information processing in biological systems, we take care to distinguish intrinsic, functional, and useful computation [53–55]. *Intrinsic computation* refers to how a physical system stores and transforms its historical information. We take *functional computation* as information processing in a physical device that promotes the performance of a larger,

- encompassing system. Whereas, we take *useful computation* as information processing in a physical device used to achieve an external user's goal. The first is well-suited to analyzing structure in physical processes and determining if they are candidate substrates for any kind of information processing. The second is well-suited for discussing biological sensors, while the third is well-suited for discussing the benefits of contemporary digital computers.
- [7] J. M. R. Parrondo, J. M. Horowitz, and T. Sagawa. Thermodynamics of information. *Nat. Physics*, 11(2):131–139, 2015.
 - [8] C. Aghamohammadi and J. P. Crutchfield. Thermodynamics of random number generation. *Phys. Rev. E*, 95(6):062139, 2017.
 - [9] M. Hinczewski and D. Thirumalai. Cellular signaling networks function as generalized Wiener-Kolmogorov filters to suppress noise. *Phys. Rev. X*, 4(4):041017, 2014.
 - [10] A. B. Boyd, D. Mandal, and J. P. Crutchfield. Correlation-powered information engines and the thermodynamics of self-correction. *Phys. Rev. E*, 95(1):012152, 2017.
 - [11] S. Still, D. A. Sivak, A. J. Bell, and G. E. Crooks. Thermodynamics of prediction. *Phys. Rev. Lett.*, 109:120604, Sep 2012.
 - [12] A. C. Barato, D. Hartich, and U. Seifert. Efficiency of cellular information processing. *New J. Physics*, 16(10):103024, 2014.
 - [13] J. M. Horowitz and M. Esposito. Thermodynamics with continuous information flow. *Phys. Rev. X*, 4:031015, Jul 2014.
 - [14] A. B. Boyd, D. Mandal, and J. P. Crutchfield. Leveraging environmental correlations: The thermodynamics of requisite variety. *J. Stat. Phys.*, 167(6):1555–1585, 2016.
 - [15] S. Goldt and U. Seifert. Stochastic thermodynamics of learning. *Phys. Rev. Lett.*, 118(1):010601, 2017.
 - [16] A. B. Boyd, D. Mandal, P. M. Riechers, and J. P. Crutchfield. Transient dissipation and structural costs of physical information transduction. *Phys. Rev. Lett.*, 118:220602, 2017.
 - [17] A. B. Boyd and J. P. Crutchfield. Maxwell demon dynamics: Deterministic chaos, the Szilard map, and the intelligence of thermodynamic systems. *Phys. Rev. Lett.*, 116:190601, 2016.
 - [18] R. P. N. Rao and D. H. Ballard. Predictive coding in the visual cortex: a functional interpretation of some extraclassical receptive-field effects. *Nat. Neurosci.*, 2(1):79–87, 1999.
 - [19] S. E. Palmer, O. Marre, M. J. Berry, and W. Bialek. Predictive information in a sensory population. *Proc. Natl. Acad. Sci. USA*, 112(22):6908–6913, 2015.
 - [20] D. B. Chklovskii and A. A. Koulakov. Maps in the brain: what can we learn from them? *Annu. Rev. Neurosci.*, 27:369–392, 2004.
 - [21] A. Hasenstaub, S. Otte, E. Callaway, and T. J. Sejnowski. Metabolic cost as a unifying principle governing neuronal biophysics. *Proc. Natl. Acad. Sci. USA*, 107(27):12329–12334, 2010.
 - [22] We only consider online or real-time computations, so that the oft-considered energy-speed-accuracy tradeoff [56, 57] reduces to an energy-accuracy tradeoff.
 - [23] R. S. Sutton and A. G. Barto. *Reinforcement learning: An introduction*. MIT Press, Cambridge, Massachusetts, 1998.
 - [24] M. L. Littman, R. S. Sutton, and S. P. Singh. In *NIPS*, volume 14, pages 1555–1561, 2001.
 - [25] N. Brodu. *Adv. Complex Sys.*, 14(05):761–794, 2011.
 - [26] D. Y. Little and F. T. Sommer. Learning and exploration in action-perception loops. *Closing the Loop Around Neural Systems*, page 295, 2014.
 - [27] N. B. Becker, A. Mugler, and P. R. ten Wolde. Optimal prediction by cellular signaling networks. *Phys. Rev. Lett.*, 115(25):258103, 2015.
 - [28] F. Creutzig and H. Sprekeler. Predictive coding and the slowness principle: An information-theoretic approach. *Neural Comp.*, 20(4):1026–1041, 2008.
 - [29] F. Creutzig, A. Globerson, and N. Tishby. Past-future information bottleneck in dynamical systems. *Phys. Rev. E*, 79(4):041925, 2009.
 - [30] S. Marzen and J. P. Crutchfield. Structure and randomness of continuous-time discrete-event processes. 2016. arxiv.org:1704.04707.
 - [31] E. M. Izhikevich. *Dynamical systems in neuroscience*. MIT press, Cambridge, Massachusetts, 2007.
 - [32] C. R. Shalizi and J. P. Crutchfield. Computational mechanics: Pattern and prediction, structure and simplicity. *J. Stat. Phys.*, 104:817–879, 2001.
 - [33] R. G. James, C. J. Ellison, and J. P. Crutchfield. Anatomy of a bit: Information in a time series observation. *CHAOS*, 21(3):037109, 2011.
 - [34] S. Still, J. P. Crutchfield, and C. J. Ellison. Optimal causal inference: Estimating stored information and approximating causal architecture. *CHAOS*, 20(3):037111, 2010.
 - [35] R. W. Yeung. A New Outlook on Shannon's Information Measures. *IEEE Trans. Info. Th.*, 37(3):466–474, 1991.
 - [36] O. L. White, D. D. Lee, and H. Sompolinsky. Short-term memory in orthogonal neural networks. *Phys. Rev. Lett.*, 92(14):148102, 2004.
 - [37] T. M. Cover and J. A. Thomas. *Elements of Information Theory*. Wiley-Interscience, New York, second edition, 2006.
 - [38] J. Schnakenberg. Network theory of microscopic and macroscopic behavior of master equation systems. *Rev. Mod. Physics*, 48(4):571, 1976.
 - [39] S. Marzen, H. G. Garcia, and R. Phillips. Statistical mechanics of monod-wyman-changeux (mwc) models. *J. Mole. Bio.*, 425(9):1433–1460, 2013.
 - [40] G. Tkačik, A. M. Walczak, and W. Bialek. Optimizing information flow in small genetic networks. *Phys. Rev. E*, 80(3):031920, 2009.
 - [41] A. M. Walczak, G. Tkačik, and W. Bialek. Optimizing information flow in small genetic networks. II. Feed-forward interactions. *Phys. Rev. E*, 81(4):041905, 2010.
 - [42] B. M. C. Martins and P. S. Swain. Trade-offs and constraints in allosteric sensing. *PLoS Comput. Bio.*,

- 7(11):e1002261, 2011.
- [43] S. Still. Information-theoretic approach to interactive learning. *EuroPhys. Lett.*, 85:28005, 2009. arxiv.org physics 0709.1948.
- [44] Naftali Tishby and Daniel Polani. Information theory of decisions and actions. In *Perception-action cycle*, pages 601–636. Springer, 2011.
- [45] S. H. Strogatz. *Nonlinear Dynamics and Chaos: with applications to physics, biology, chemistry, and engineering*. Addison-Wesley, Reading, Massachusetts, 1994.
- [46] C. T. Bergstrom and M. Lachmann. Shannon information and biological fitness. In *Information Theory Workshop, 2004. IEEE*, volume IEEE 0-7803-8720-1, pages 50–54. IEEE, 2004.
- [47] M. G. Bulmer. Delayed germination of seeds: Cohen’s model revisited. *Theo. Pop. Bio.*, 26:367–377, 1984.
- [48] S. Maslov and K. Sneppen. Well-temperate phage: optimal bet-hedging against local environmental collapses. *Sci. Reports*, 5:10523, 2015.
- [49] D. Cohen. Optimizing reproduction in a randomly varying environment. *J. Theo. Bio.*, 12:119–129, 1966.
- [50] J. A. J. Metz, R. M. Nisbet, and S. A. H. Geritz. How should we define fitness for general ecological scenarios? *Trends Ecol. Evol.*, 7:198–202, 1992.
- [51] J. Seger and H. J. Brockmann. What is bet-hedging? *Oxford Surveys in Evolutionary Biology*, 4:182–211, 1987.
- [52] L. Arnold. *Random dynamical systems*. Springer Science & Business Media, New York, New York, 2013.
- [53] J. P. Crutchfield and K. Young. Inferring statistical complexity. *Phys. Rev. Lett.*, 63:105–108, 1989.
- [54] J. P. Crutchfield. The calculi of emergence: Computation, dynamics, and induction. *Physica D*, 75:11–54, 1994.
- [55] J. P. Crutchfield and M. Mitchell. The evolution of emergent computation. *Proc. Natl. Acad. Sci.*, 92:10742–10746, 1995.
- [56] G. Lan, P. Sartori, S. Neumann, V. Sourjik, and Y. Tu. The energy-speed-accuracy trade-off in sensory adaptation. *Nat. Physics*, 8(5):422–428, 2012.
- [57] S. Lahiri, J. Sohl-Dickstein, and S. Ganguli. A universal tradeoff between power, precision and speed in physical communication. *arXiv:1603.07758*, 2016.

Supplementary Materials
Prediction and Power in Molecular Sensors
 Sarah E. Marzen and James P. Crutchfield

I. EXTENDING KELLY'S ARGUMENT

Although the use of mutual information for a biological sensor may seem arbitrary, it gains operational significance via a straightforward extension of Kelly's bet-hedging arguments [37, Ch. 6 of]. Here, we switch to a discrete-time analysis. Kelly's classic result states that a population of organisms increases its expected log growth rate by $I[Y_t; X_{t+1}]$ —the *instantaneous predictive information*. Each organism stores information about the past environments in a sensory variable y and chooses stochastically from $p(g|y)$ to exhibit phenotype g based on this sensory variable. Kelly's original derivation assumed that only one phenotype can reproduce in each possible environment. We extend this result by relaxing this assumption, following Ref. [46]. Let n_t be the number of organisms at time t ; let $p(g|y_t)$ be the probability that an organism expresses phenotype g given sensory state y_t ; let x_t be the sensory input at time t ; and let $f(g, x)$ be the growth rate of phenotype g in environment x . Then, we straightforwardly obtain:

$$\begin{aligned} n_{t+1} &= \sum_g (p(g|y_t)n_t)f(g, x_{t+1}) \\ &= \left(\sum_g p(g|y_t)f(g, x_{t+1}) \right) n_t . \end{aligned}$$

This yields an expected log growth rate of:

$$\begin{aligned} r &= \left\langle \log \frac{n_{t+1}}{n_t} \right\rangle \\ &= \left\langle \log \left(\sum_g p(g|y_t)f(g, x_{t+1}) \right) \right\rangle \\ &= \sum_{y_t, x_{t+1}} p(y_t, x_{t+1}) \log \left(\sum_g p(g|y_t)f(g, x_{t+1}) \right) . \end{aligned}$$

We seek the bet-hedging strategy that maximizes expected log growth rate. That is, maximize r , subject to the constraint that $\sum_g p(g|y_t) = 1$ for all y_t , via the Lagrangian:

$$\begin{aligned} \mathcal{L} &= \sum_{y_t, x_{t+1}} p(y_t, x_{t+1}) \log \left(\sum_g p(g|y_t)f(g, x_{t+1}) \right) \\ &\quad + \sum_{y_t} \lambda_{y_t} \sum_g p(g|y_t) , \end{aligned}$$

with respect to $p(g|y_t)$. Following Ref. [46], let \mathbf{x} be the vector of optimal $p(g|y_t)$, let \mathbf{p} be the vector of $p(x|y_t)$, and let W be the matrix with elements $f(g, x)$. Then, we find that:

$$\begin{aligned} (W\mathbf{x})_k &= p_k / \sum_j (W^{-1})_{jk} \\ \rightarrow \mathbf{x} &= W^{-1} (\mathbf{p} \odot [\mathbf{1}^\top W^{-1}]^{\odot -1}) \end{aligned}$$

is the maximizing conditional distribution *if* it is in the interior of the simplex. This gives an expected log growth rate:

$$\begin{aligned} r^* &= \sum_{y_t, x_{t+1}} p(y_t, x_{t+1}) \log \frac{p(x_{t+1}|y_t)}{\sum_g (W^{-1})_{g, x_{t+1}}} \\ &= -H[X_{t+1}|Y_t] - \sum_{x_{t+1}} p(x_{t+1}) \log \sum_g ((W^{-1})_{g, x_{t+1}}) . \end{aligned}$$

The difference between this expected log growth rate and the maximal expected log growth rate of a population without any sensing capabilities is:

$$\begin{aligned} \Delta r^* &= -H[X_{t+1}|Y_t] + H[X_{t+1}] \\ &= I[Y_t; X_{t+1}] . \end{aligned} \tag{S1}$$

This is exactly the instantaneous predictive information, which lower bounds the total predictable information calculated here.

II. REVISITING THE ‘‘THERMODYNAMICS OF PREDICTION’’

For completeness, we review the derivation of Eq. (5). Let x_t represent the input at time t , let y_t represent the sensor state at time t , and let $E(x, y)$ denote the system's energy function. We assume constant temperature. The system's temperature-normalized nonequilibrium free energy F_{neq} is given by:

$$\beta F_{neq}[p(x, y)] = \beta \langle E(x, y) \rangle - H[Y|X] . \tag{S2}$$

The validity of Ref. [11]'s derivation rests on the nonequilibrium free energy being a Lyapunov function. Intuitively, this corresponds to an assumption that the system reduces its nonequilibrium free energy when the sensor thermalizes. If so, then:

$$\beta F_{neq}[p(x_{t+\Delta t}, y_t)] \geq \beta F_{neq}[p(x_{t+\Delta t}, y_{t+\Delta t})] ,$$

giving:

$$\begin{aligned} 0 &\leq \beta F_{neq}[p(x_{t+\Delta t}, y_t)] - \beta F_{neq}[p(x_{t+\Delta t}, y_{t+\Delta t})] \\ &\leq (\beta \langle E(x_{t+\Delta t}, y_t) \rangle - H[Y_t | X_{t+\Delta t}]) \\ &\quad - (\beta \langle E(x_{t+\Delta t}, y_{t+\Delta t}) \rangle - H[Y_{t+\Delta t} | X_{t+\Delta t}]) \end{aligned}$$

and, from stationarity, $\langle E(x_{t+\Delta t}, y_{t+\Delta t}) \rangle = \langle E(x_t, y_t) \rangle$ and $H[Y_{t+\Delta t} | X_{t+\Delta t}] = H[Y_t | X_t]$, giving:

$$\begin{aligned} 0 &\leq \beta (\langle E(x_{t+\Delta t}, y_t) \rangle - \langle E(x_t, y_t) \rangle) \\ &\quad - (H[Y_t | X_{t+\Delta t}] - H[Y_t | X_t]) \\ &\leq \lim_{\Delta t \rightarrow 0} \frac{\beta (\langle E(x_{t+\Delta t}, y_t) \rangle - \langle E(x_t, y_t) \rangle)}{\Delta t} \\ &\quad - \lim_{\Delta t \rightarrow 0} \frac{H[Y_t | X_{t+\Delta t}] - H[Y_t | X_t]}{\Delta t} . \end{aligned}$$

We recognize the first term as the temperature-normalized power βP . Hence, the nonpredictive information rate is the increase in unpredictability of sensor state Y_t given a slightly delayed environmental state:

$$\dot{I}_{\text{np}} := \lim_{\Delta t \rightarrow 0} \frac{H[Y_t | X_{t+\Delta t}] - H[Y_t | X_t]}{\Delta t} \leq \beta P . \quad (\text{S3})$$

From standard information theory identities [37]—namely, $I[U; V] = H[U] - H[U|V]$ —we see that:

$$H[Y_t | X_{t+\Delta t}] - H[Y_t | X_t] = I[Y_t; X_t] - I[Y_t; X_{t+\Delta t}] .$$

Reference [11]’s main result follows directly:

$$\dot{I}_{\text{np}} = \lim_{\Delta t \rightarrow 0} \frac{I[Y_t; X_t] - I[Y_t; X_{t+\Delta t}]}{\Delta t} \leq \beta P . \quad (\text{S4})$$

Differences in presentation come from the difference between discrete- and continuous-time formulations. To make this clear, we present a continuous-time formula-

tion of the same result, following Ref. [13]. We start from $\beta F_{neq}[p(x_t, y_{t'})]$ being a Lyapunov function in t' :

$$\begin{aligned} 0 &\geq \beta \frac{\partial F_{neq}[p(x_t, y_{t'})]}{\partial t'} \\ &= \beta \frac{\partial}{\partial t'} \langle E(x_t, y_{t'}) \rangle \Big|_{t'=t} - \frac{\partial}{\partial t'} H[Y_{t'} | X_t] \Big|_{t'=t} \\ &= \beta \left\langle \frac{\partial E(x_t, y_t)}{\partial y_t} \dot{y}_t \right\rangle - \frac{\partial}{\partial t'} H[Y_{t'} | X_t] \Big|_{t'=t} . \end{aligned}$$

We then recognize $\beta \left\langle \frac{\partial E(x_t, y_t)}{\partial y_t} \dot{y}_t \right\rangle$ as the temperature-normalized rate of heat dissipation $\beta \dot{Q}$, so that:

$$\beta \dot{Q} \leq \frac{\partial}{\partial t'} H[Y_{t'} | X_t] \Big|_{t'=t} .$$

In nonequilibrium steady state, $\frac{d}{dt} \langle E \rangle = 0$ and $\frac{d}{dt} H[Y_t | X_t] = 0$. As a result, $\beta \dot{Q} + \beta P = 0$ and:

$$\frac{\partial}{\partial t'} H[Y_{t'} | X_t] \Big|_{t'=t} = - \frac{\partial}{\partial t'} H[Y_t | X_{t'}] \Big|_{t'=t} ,$$

giving:

$$\beta P \geq \frac{\partial}{\partial t'} H[Y_t | X_{t'}] \Big|_{t'=t} , \quad (\text{S5})$$

which we recognize as the continuous-time formulation of Eq. (S3). Again invoking stationarity, $\frac{d}{dt} H[X_t] = 0$, and so:

$$\beta P \geq - \frac{\partial}{\partial t'} I[X_{t'}; Y_t] \Big|_{t'=t} , \quad (\text{S6})$$

the continuous-time formulation of Eq. (S4). We have, in Eqs. (S3), (S4), (S5), and (S6), four equivalent definitions for the nonpredictive information rate in the nonequilibrium steady state limit.

III. CLOSED-FORM EXPRESSIONS FOR UNIFILAR HIDDEN SEMI-MARKOV ENVIRONMENTS

To find $\rho(\sigma^+, y)$, we start with the following:

$$\begin{aligned} \Pr(\mathcal{S}_{t+\Delta t}^+ = (g, x, \tau), Y_{t+\Delta t} = y) \\ = \sum_{g', x', \tau', y'} \Pr(\mathcal{S}_{t+\Delta t}^+ = (g, x, \tau), Y_{t+\Delta t} = y | \mathcal{S}_t^+ = (g', x', \tau'), Y_t = y') \Pr(\mathcal{S}_t^+ = (g', x', \tau'), Y_t = y') . \end{aligned} \quad (\text{S7})$$

We decompose the transition probability using the feedforward nature of the transducer as:

$$\begin{aligned} \Pr(\mathcal{S}_{t+\Delta t}^+ = (g, x, \tau), Y_{t+\Delta t} = y | \mathcal{S}_t^+ = (g', x', \tau'), Y_t = y') &= \Pr(\mathcal{S}_{t+\Delta t}^+ = (g, x, \tau) | \mathcal{S}_t^+ = (g', x', \tau')) \\ &\quad \times \Pr(Y_{t+\Delta t} = y | \mathcal{S}_t^+ = (g', x', \tau'), Y_t = y') . \end{aligned}$$

From the setup, we have:

$$\Pr(Y_{t+\Delta t} = y | \mathcal{S}_t^+ = (g', x', \tau'), Y_t = y') = \begin{cases} k_{y' \rightarrow y}(x') \Delta t & y \neq y' \\ 1 - k_{y' \rightarrow y'}(x') \Delta t & y = y' \end{cases},$$

with corrections of $O(\Delta t^2)$.

Now split this into two cases. As long as $\tau > \Delta t$, so that $x = x'$, we have:

$$\Pr(\mathcal{S}_{t+\Delta t}^+ = (g, x, \tau) | \mathcal{S}_t^+ = (g', x', \tau')) = \frac{\Phi_g(\tau)}{\Phi_g(\tau')} \delta(\tau - (\tau' + \Delta t)) \delta_{x, x'} \delta_{g, g'}.$$

Then, Eq. (S7) reduces to

$$\begin{aligned} \Pr(\mathcal{S}_{t+\Delta t}^+ = (g, x, \tau), Y_{t+\Delta t} = y) &= \sum_{y'} \Pr(\mathcal{S}_{t+\Delta t}^+ = (g, x, \tau) | \mathcal{S}_t^+ = (g, x, \tau - \Delta t)) \Pr(Y_{t+\Delta t} = y | \mathcal{S}_t^+ = (g, x, \tau - \Delta t), Y_t = y') \\ &\quad \times \Pr(\mathcal{S}_t^+ = (g, x, \tau - \Delta t), Y_t = y') \\ &= \sum_{y' \neq y} \Pr(\mathcal{S}_{t+\Delta t}^+ = (g, x, \tau) | \mathcal{S}_t^+ = (g, x, \tau - \Delta t)) \Pr(Y_{t+\Delta t} = y | \mathcal{S}_t^+ = (g, x, \tau - \Delta t), Y_t = y') \\ &\quad \times \Pr(\mathcal{S}_t^+ = (g, x, \tau - \Delta t), Y_t = y') \\ &\quad + \Pr(\mathcal{S}_{t+\Delta t}^+ = (g, x, \tau) | \mathcal{S}_t^+ = (g, x, \tau - \Delta t)) \Pr(Y_{t+\Delta t} = y | \mathcal{S}_t^+ = (g, x, \tau - \Delta t), Y_t = y) \\ &\quad \times \Pr(\mathcal{S}_t^+ = (g, x, \tau - \Delta t), Y_t = y) \\ &= \sum_{y' \neq y} \frac{\Phi_g(\tau)}{\Phi_g(\tau - \Delta t)} k_{y' \rightarrow y}(x) \Pr(\mathcal{S}_t^+ = (g, x, \tau - \Delta t), Y_t = y') \Delta t \\ &\quad + \frac{\Phi_g(\tau)}{\Phi_g(\tau - \Delta t)} (1 - k_{y \rightarrow y}(x) \Delta t) \Pr(\mathcal{S}_t^+ = (g, x, \tau - \Delta t), Y_t = y), \end{aligned} \quad (\text{S8})$$

plus terms of $O(\Delta t^2)$. We Taylor expand $\Phi_g(\tau + \Delta t) = \Phi_g(\tau) - \phi_g(\tau) \Delta t$ to find:

$$\frac{\Phi_g(\tau)}{\Phi_g(\tau - \Delta t)} = 1 - \frac{\phi_g(\tau)}{\Phi_g(\tau)} \Delta t,$$

plus terms of $O(\Delta t^2)$. And, similarly, assuming differentiability, we write:

$$\Pr(\mathcal{S}_t^+ = (g, x, \tau - \Delta t), Y_t = y') = \Pr(\mathcal{S}_t^+ = (g, x, \tau), Y_t = y') - \frac{d}{d\tau} \Pr(\mathcal{S}_t^+ = (g, x, \tau), Y_t = y') \Delta t,$$

plus terms of $O(\Delta t^2)$. Substitution into Eq. (S8) then gives:

$$\begin{aligned} \Pr(\mathcal{S}_{t+\Delta t}^+ = (g, x, \tau), Y_{t+\Delta t} = y) &= \left(\sum_{y' \neq y} k_{y' \rightarrow y}(x) \Pr(\mathcal{S}_t^+ = (g, x, \tau), Y_t = y') \right) \Delta t + \Pr(\mathcal{S}_t^+ = (g, x, \tau), Y_t = y) \\ &\quad - \frac{d \Pr(\mathcal{S}_t^+ = (g, x, \tau), Y_t = y)}{d\tau} \Delta t - \frac{\phi_g(\tau)}{\Phi_g(\tau)} \Pr(\mathcal{S}_t^+ = (g, x, \tau), Y_t = y) \Delta t \\ &\quad - k_{y \rightarrow y}(x) \Pr(\mathcal{S}_t^+ = (g, x, \tau), Y_t = y) \Delta t, \end{aligned}$$

plus terms of $O(\Delta t^2)$. For notational ease, we denote:

$$\rho((g, x, \tau), y) := \Pr(\mathcal{S}_t^+ = (x, \tau), Y_t = y),$$

which is equal to $\Pr(\mathcal{S}_{t+\Delta t}^+ = (g, x, \tau), Y_{t+\Delta t} = y)$ since we assumed the system is in a NESS. Then we have:

$$\begin{aligned} \rho((g, x, \tau), y) &= \left(\sum_{y' \neq y} k_{y' \rightarrow y}(x) \rho((g, x, \tau), y') \right) \Delta t + \rho((g, x, \tau), y) - \frac{d\rho((g, x, \tau), y)}{d\tau} \Delta t \\ &\quad - \frac{\phi_g(\tau)}{\Phi_g(\tau)} \rho((g, x, \tau), y) \Delta t - k_{y \rightarrow y}(x) \rho((g, x, \tau), y) \Delta t \end{aligned}$$

plus corrections of $O(\Delta t^2)$. We are left equating the coefficient of the $O(\Delta t)$ term to 0:

$$\frac{d\rho((g, x, \tau), y)}{d\tau} = \sum_{y' \neq y} k_{y' \rightarrow y}(x) \rho((g, x, \tau), y') - \frac{\phi_g(\tau)}{\Phi_g(\tau)} \rho((g, x, \tau), y) - k_{y \rightarrow y}(x) \rho((g, x, \tau), y) . \quad (\text{S9})$$

Our task is simplified if we separate:

$$\rho((g, x, \tau), y) = p(y|g, x, \tau) \rho(g, x, \tau)$$

and if we recall that;

$$\rho(g, x, \tau) = \mu_g \Phi_g(\tau) p(g) p(x|g) .$$

These give:

$$\frac{d\rho(g, x, \tau)}{d\tau} = -\mu_g \phi_g(\tau) p(x) p(x|g) . \quad (\text{S10})$$

Plugging Eq. (S10) into Eq. (S9) yields:

$$\begin{aligned} \frac{dp(y|x, \tau)}{d\tau} \rho(g, x, \tau) - \mu_g \phi_g(\tau) p(g) p(x|g) p(y|g, x, \tau) \\ = \sum_{y' \neq y} k_{y' \rightarrow y}(x) \rho(g, x, \tau) p(y'|g, x, \tau) - \frac{\phi_g(\tau)}{\Phi_g(\tau)} \rho(g, x, \tau) p(y|g, x, \tau) - k_{y \rightarrow y}(x) \rho(g, x, \tau) p(y|g, x, \tau) , \end{aligned}$$

where we note that:

$$\mu_g \phi_g(\tau) p(g) p(x|g) p(y|g, x, \tau) = \frac{\phi_g(\tau)}{\Phi_g(\tau)} \rho(g, x, \tau) p(y|g, x, \tau) .$$

Hence, we are left with:

$$\frac{dp(y|g, x, \tau)}{d\tau} = \sum_{y' \neq y} k_{y' \rightarrow y}(x) p(y'|g, x, \tau) - k_{y \rightarrow y}(x) p(y|g, x, \tau) .$$

We can summarize this ordinary differential equation in matrix-vector notation as follows. Let $\vec{v}(g, x, \tau)$ be the vector:

$$\vec{v}(g, x, \tau) := \begin{pmatrix} p(y_1|g, x, \tau) \\ \vdots \\ p(y_{|\mathcal{Y}|}|g, x, \tau) \end{pmatrix} .$$

We have:

$$\frac{d\vec{v}}{d\tau} = M(x) \vec{v} .$$

The solution to the equation above is:

$$\vec{v}(g, x, \tau) = e^{M(x)\tau} \vec{v}(g, x, 0) . \quad (\text{S11})$$

The structure of $M(x)$ guarantees that probability is conserved, as long as $1^\top \vec{v}(g, x, 0) = 1$ for all $x \in \mathcal{A}$.

Our next task is to find expressions for $\vec{v}(g, x, 0)$. We do this by considering Eq. (S7) in the limit that $\tau < \Delta t$. More straightforwardly, we consider the equation:

$$\rho((g, x, 0), y) = \sum_{g', x'} \int_0^\infty d\tau \frac{\phi_{g'}(\tau)}{\Phi_{g'}(\tau)} \delta_{g, \epsilon+(g', x')} p(x|g) \rho((g', x', \tau), y) , \quad (\text{S12})$$

which is based on the following logic. For probability to flow into $\rho((g, x, 0), y)$ from $\rho((g', x', \tau), y')$, we need the dwell time for symbol x' to be exactly τ and for $y' = y$. (The latter comes from the unlikelihood of switching both channel state and input symbol at the same time.) Again decomposing:

$$\begin{aligned} \rho((g', x', \tau), y) &= p(y|g', x', \tau) \rho(g', x', \tau) \\ &= \mu_{g'} \Phi_{g'}(\tau) p(g') p(x'|g') p(y|g', x', \tau) \end{aligned} \quad (\text{S13})$$

and, thus, as a special case:

$$\rho((g, x, 0), y) = p(y|g, x, 0) p(g) p(x|g) \mu_g . \quad (\text{S14})$$

Plugging both Eqs. (S13) and (S14) into Eq. (S12), we find:

$$\begin{aligned} \mu_g p(g) p(x|g) p(y|g, x, 0) &= \sum_{g', x'} \int_0^\infty \mu_{g'} p(g') p(x'|g') \phi_{g'}(\tau) \delta_{g, \epsilon+(g', x')} p(x|g) p(y|g', x', \tau) d\tau \\ \mu_g p(g) p(y|g, x, 0) &= \sum_{g', x'} \int_0^\infty \mu_{g'} p(g') p(x'|g') \phi_{g'}(\tau) \delta_{g, \epsilon+(g', x')} p(y|g', x', \tau) d\tau . \end{aligned}$$

Using Eq. (S11), we see that $p(y|g', x', \tau) = \left(e^{M(x')\tau} \vec{v}(g', x', 0) \right)_y$ and $p(y|g, x, 0) = \left(\vec{v}(g, x, 0) \right)_y$. So, we have:

$$\mu_g p(g) \vec{v}(g, x, 0) = \sum_{g', x'} \mu_{g'} \delta_{g, \epsilon+(g', x')} p(g') p(x'|g') \left(\int_0^\infty \phi_{g'}(\tau) e^{M(x')\tau} d\tau \right) \vec{v}(g', x', 0) .$$

If we form the composite vector \vec{V} as:

$$\begin{aligned} \vec{V} &= \begin{pmatrix} \vec{u}(g_1, x_1) \\ \vec{u}(g_1, x_2) \\ \vdots \\ \vec{u}(g_{|\mathcal{G}|}, x_{|\mathcal{A}|}) \end{pmatrix} \\ &:= \begin{pmatrix} \mu_{g_1} p(g_1) \vec{v}(g_1, x_1, 0) \\ \vdots \\ \mu_{g_{|\mathcal{G}|}} p(g_{|\mathcal{G}|}) \vec{v}(g_{|\mathcal{G}|}, x_{|\mathcal{A}|}, 0) \end{pmatrix} \end{aligned}$$

and the matrix (written in block form) as:

$$\mathbf{C} := \begin{pmatrix} C_{(g_1, x_1) \rightarrow (g_1, x_1)} & C_{(g_1, x_2) \rightarrow (g_1, x_1)} & \cdots \\ C_{(g_1, x_1) \rightarrow (g_1, x_2)} & C_{(g_1, x_2) \rightarrow (g_1, x_2)} & \cdots \\ \vdots & \vdots & \ddots \end{pmatrix} ,$$

with:

$$C_{(g',x') \rightarrow (g,x)} = \delta_{g,\epsilon^+(g',x')} p(x'|g') \int_0^\infty \phi_{g'}(t) e^{M(x')t} dt ,$$

we then have:

$$\vec{U} = \text{eig}_1(\mathbf{C}) . \quad (\text{S15})$$

Finally, we must normalize $\vec{u}(x)$ appropriately. We do this by recalling that $\mathbf{1}^\top \vec{v}(g, x, 0) = 1$, since $\vec{v}(g, x, 0)$ is a vector of probabilities. Then we have:

$$\vec{u}(g, x) \rightarrow \frac{\vec{u}(g, x)}{\mathbf{1}^\top \vec{u}(g, x)} \mu_g p(g) .$$

for each g, x .

To calculate predictive metrics—i.e., I_{mem} and I_{fut} —we need $p(x, y)$ and $p(y, \sigma^-)$. The former is a marginalization of $p(\sigma^+, y)$ that we just calculated. The second can be calculated via:

$$p(\sigma^-, y) = \sum_{\sigma^+} p(\sigma^- | \sigma^+) p(y, \sigma^+) ,$$

where

$$\begin{aligned} p(\sigma^- | \sigma^+) &= p((g_-, x_-, \tau_-) | (g_+, x_+, \tau_+)) \\ &= \delta_{x_+, x_-} p(g_- | g_+, x_+) \mu_{g_+} \phi_{g_+}(\tau_+ + \tau_-) . \end{aligned}$$

Hence, we turn our attention to dissipative metrics.

For calculation of dissipative metrics, we only need:

$$\frac{\delta p}{\delta t} = \lim_{\Delta t \rightarrow 0} \frac{\Pr(X_{t+\Delta t} = x, Y_t = y) - \Pr(X_t = x, Y_t = y)}{\Delta t} .$$

Moreover, we can use the Markov chain $Y_t \rightarrow \mathcal{S}_t^+ \rightarrow X_{t+\Delta t}$ to compute it:

$$\Pr(X_{t+\Delta t} = x, Y_t = y) = \sum_{\sigma^+} \Pr(X_{t+\Delta t} = x | \mathcal{S}_t^+ = \sigma^+) \Pr(Y_t = y, \mathcal{S}_t^+ = \sigma^+) .$$

We have:

$$\begin{aligned} \Pr(X_{t+\Delta t} = x | \mathcal{S}_t^+ = \sigma^+) &= \Pr(X_{t+\Delta t} = x | \mathcal{S}_t^+ = (g', x', \tau')) \\ &= \begin{cases} \frac{\Phi_{g'}(\tau' + \Delta t)}{\Phi_{g'}(\tau')} & x = x' \\ \frac{\phi_{g'}(\tau')}{\Phi_{g'}(\tau')} p(x | \epsilon^+(g', x')) \Delta t & x \neq x' \end{cases} . \end{aligned}$$

This, combined with $p(\sigma^+, y)$, gives:

$$\begin{aligned}
\Pr(X_{t+\Delta t} = x, Y_t = y) &= \sum_{g', x' \neq x} \int d\tau' \rho((g', x', \tau'), y) \frac{\phi_{g'}(\tau')}{\Phi_{g'}(\tau')} \Delta t p(x|\epsilon^+(g', x')) \\
&\quad + \sum_{g'} \int d\tau' \frac{\Phi_{g'}(\tau' + \Delta t)}{\Phi_{g'}(\tau')} \rho((g', x', \tau'), y) \\
&= \Pr(X_t = x, Y_t = y) + \Delta t \left(\sum_{g', x' \neq x} \int d\tau' p(x|\epsilon^+(g', x')) \frac{\phi_{g'}(\tau')}{\Phi_{g'}(\tau')} \rho((g', x', \tau'), y) \right. \\
&\quad \left. - \sum_{g'} \int d\tau' \frac{\phi_{g'}(\tau')}{\Phi_{g'}(\tau')} \rho((g', x, \tau'), y) \right),
\end{aligned}$$

correct to $O(\Delta t)$. Recalling that:

$$\begin{aligned}
\rho((g', x', \tau'), y) &= \rho(g', x', \tau') p(y|g', x', \tau') \\
&= p(x'|g') \Phi_{g'}(\tau') \left(e^{M(x')\tau'} \vec{u}(g', x') \right)_y,
\end{aligned}$$

gives:

$$\begin{aligned}
\frac{\delta p}{\delta t} &= \lim_{\Delta t \rightarrow 0} \frac{\Pr(X_{t+\Delta t} = x, Y_t = y) - \Pr(X_t = x, Y_t = y)}{\Delta t} \\
&= \sum_{g', x' \neq x} \int d\tau' p(x|\epsilon^+(g', x')) \frac{\phi_{g'}(\tau')}{\Phi_{g'}(\tau')} \rho((g', x', \tau'), y) - \sum_{g'} \int d\tau' \frac{\phi_{g'}(\tau')}{\Phi_{g'}(\tau')} \rho((g', x, \tau'), y) \quad (\text{S16})
\end{aligned}$$

$$\begin{aligned}
&= \sum_{g', x' \neq x} \int d\tau' p(x|\epsilon^+(g', x')) p(x'|g') \phi_{g'}(\tau') \left(e^{M(x')\tau'} \vec{u}(g', x') \right)_y \\
&\quad - \sum_{g'} \int d\tau' p(x|g') \phi_{g'}(\tau') \left(e^{M(x)\tau'} \vec{u}(g', x) \right)_y. \quad (\text{S17})
\end{aligned}$$

From this, Eqs. (8) and (11) can be used to calculate \dot{I}_{np} and βP .

IV. SPECIALIZATION TO SEMI-MARKOV INPUT

Up to this point, we wrote expressions for the general case of unifilar hidden semi-Markov input. We now specialize to the semi-Markov input case. A great simplification ensues: hidden states g are the current emitted symbols x . Recall that, in an abuse of notation, $q(x|x')$ is now the probability of observing symbol x after seeing symbol x' .

Hence, forward-time causal states are given by the pair (x, τ) . The analog of Eq. (S11) is:

$$\vec{p}(y|x, \tau) = e^{M(x)\tau} \vec{p}(y|x, 0),$$

and we define vectors:

$$\vec{u}(x) := \mu_x p(x) \vec{p}(y|x, 0).$$

The large vector:

$$\vec{U} := \begin{pmatrix} \vec{u}(x_1) \\ \vdots \\ \vec{u}(x_{|\mathcal{A}|}) \end{pmatrix}$$

is the eigenvector $\text{eig}_1(\mathbf{C})$ of eigenvalue 1 of the matrix:

$$\mathbf{C} = \begin{pmatrix} 0 & q(x_1|x_2) \int_0^\infty \phi_{x_2}(\tau) e^{M(x_2)\tau} d\tau & & & \\ \dots & & & & \\ q(x_2|x_1) \int_0^\infty \phi_{x_1}(\tau) e^{M(x_1)\tau} d\tau & & & & \\ \dots & & & & \\ \vdots & & & \vdots & \ddots \end{pmatrix},$$

where normalization requires $1^\top \vec{u}(x) = \mu_x p(x)$.

We continue by finding $p(y)$, since from this we obtain $\mathbf{H}[Y]$. We do this via straightforward marginalization:

$$\begin{aligned} p(y) &= \sum_{\sigma^+} \rho(\sigma^+, y) = \sum_{\sigma^+} p(y|\sigma^+) \rho(\sigma^+) \\ &= \sum_x \int_0^\infty p(y|x, \tau) \rho(x, \tau) d\tau \\ &= \sum_x \int_0^\infty \left(e^{M(x)\tau} \vec{v}(x, 0) \right)_y \mu_x p(x) \Phi_x(\tau) d\tau \\ &= \sum_x \left(\left(\int_0^\infty e^{M(x)\tau} \Phi_x(\tau) d\tau \right) \vec{u}(x) \right)_y. \end{aligned}$$

This implies that:

$$\vec{p}(y) = \sum_x \left(\int_0^\infty e^{M(x)\tau} \Phi_x(\tau) d\tau \right) \vec{u}(x).$$

From earlier, recall that $\vec{u}(x) := \mu_x p(x) \vec{p}(y|x, 0)$.

Next, we aim to find $p(x, y)$, again via marginalization:

$$\begin{aligned} p(x, y) &= \int_0^\infty \rho((x, \tau), y) d\tau \\ &= \int_0^\infty \mu_x p(x) \Phi_x(\tau) p(y|x, \tau) d\tau \\ &= \int_0^\infty \mu_x p(x) \Phi_x(\tau) \left(e^{M(x)\tau} \vec{v}(x, 0) \right)_y d\tau \\ &= \left(\left(\int_0^\infty e^{M(x)\tau} \Phi_x(\tau) d\tau \right) \vec{u}(x) \right)_y. \end{aligned} \tag{S18}$$

From the joint distribution $p(x, y)$, we easily numerically obtain $\mathbf{I}[X; Y]$, since $|\mathcal{A}| < \infty$ and $|\mathcal{Y}| < \infty$.

For notational ease, we introduced \mathcal{T}_t in this section as the random variable for the time since last symbol, whose realization is τ . Finally, we require $p(y|\sigma^-)$ to calculate $\mathbf{H}[Y|\mathcal{S}^-]$, which we can then combine with $\mathbf{H}[Y]$ to get an estimate for \mathbf{I}_{fut} . We utilize the Markov chain $Y \rightarrow \mathcal{S}^+ \rightarrow \mathcal{S}^-$, as stated earlier, and so have:

$$\begin{aligned} p(y|\sigma^-) &= \sum_{\sigma^+} \rho(y, \sigma^+|\sigma^-) \\ &= \sum_{\sigma^+} p(y|\sigma^+, \sigma^-) \rho(\sigma^+|\sigma^-) \\ &= \sum_{\sigma^+} p(y|\sigma^+) \rho(\sigma^+|\sigma^-). \end{aligned}$$

Eq. (S11) gives us $p(y|\sigma^+)$ as:

$$\begin{aligned} p(y|\sigma^+) &= p(y|x_+, \tau_+) \\ &= \left(e^{M(x_+)\tau_+} \vec{v}(x_+, 0) \right)_y \end{aligned}$$

and Eq. (2) gives us $\rho(\sigma^+|\sigma^-)$ after some manipulation:

$$\begin{aligned} \rho(\sigma^+|\sigma^-) &= \rho((x_+, \tau_+)|(x_-, \tau_-)) \\ &= \delta_{x_+, x_-} \frac{\phi_{x_-}(\tau_+ + \tau_-)}{\Phi_{x_-}(\tau_-)}. \end{aligned}$$

Combining the two equations gives:

$$\begin{aligned} p(y|x_-, \tau_-) &= \sum_{x_+} \int_0^\infty \delta_{x_+, x_-} \frac{\phi_{x_-}(\tau_+ + \tau_-)}{\Phi_{x_-}(\tau_-)} \left(e^{M(x_+)\tau_+} \vec{v}(x_+, 0) \right)_y d\tau_+ \\ &= \frac{1}{\Phi_{x_-}(\tau_-)} \left(\left(\int_0^\infty \phi_{x_-}(\tau_+ + \tau_-) e^{M(x_-)\tau_+} d\tau_+ \right) \vec{v}(x_-, 0) \right)_y. \end{aligned}$$

From this conditional distribution, we compute $H[Y|\mathcal{S}^- = \sigma^-]$, and so $H[Y|\mathcal{S}^-] = \langle H[Y|\mathcal{S}^- = \sigma^-] \rangle_{\rho(\sigma^-)}$. In more detail, define:

$$D_x(\tau) := \int_0^\infty \phi_x(\tau + s) e^{M(x)s} ds,$$

and we have:

$$\vec{p}(y|x_-, \tau_-) = D_{x_-}(\tau_-) \vec{u}(x_-) / \mu_{x_-} p(x_-) \Phi_{x_-}(\tau_-).$$

This conditional distribution gives:

$$\begin{aligned} H[Y|X_- = x_-, \mathcal{T}_- = \tau_-] &= - \sum_y p(y|x_-, \tau_-) \log p(y|x_-, \tau_-) \\ &= -1^\top \left(\frac{D_{x_-}(\tau_-) \vec{u}(x_-)}{\mu_{x_-} p(x_-) \Phi_{x_-}(\tau_-)} \log \left(\frac{D_{x_-}(\tau_-) \vec{u}(x_-)}{\mu_{x_-} p(x_-) \Phi_{x_-}(\tau_-)} \right) \right) \\ &= - \frac{1}{\mu_{x_-} p(x_-) \Phi_{x_-}(\tau_-)} \left(1^\top ((D_{x_-}(\tau_-) \vec{u}(x_-)) \log(D_{x_-}(\tau_-) \vec{u}(x_-))) \right. \\ &\quad \left. - 1^\top (D_{x_-}(\tau_-) \vec{u}(x_-)) \log(\mu_{x_-} p(x_-) \Phi_{x_-}(\tau_-)) \right). \end{aligned}$$

We recognize the factor $\mu_{x_-} p(x_-) \Phi_{x_-}(\tau_-)$ as $\rho(x_-, \tau_-)$ and so we find that:

$$\begin{aligned} H[Y|X_-, \mathcal{T}_-] &= \sum_{x_-} \int_0^\infty \rho(x_-, \tau_-) H[Y|X_- = x_-, \mathcal{T}_- = \tau_-] d\tau_- \\ &= - \int_0^\infty \left(\sum_{x_-} 1^\top ((D_{x_-}(\tau_-) \vec{u}(x_-)) \log(D_{x_-}(\tau_-) \vec{u}(x_-))) \right) d\tau_- \\ &\quad + \int_0^\infty \left(\sum_{x_-} 1^\top D_{x_-}(\tau_-) \vec{u}(x_-) \log(\mu_{x_-} p(x_-) \Phi_{x_-}(\tau_-)) \right) d\tau_-. \end{aligned}$$

This, combined with earlier formula for $H[Y]$, gives I_{fut} .

Finally, we wish to find an expression for the nonpredictive information rate \dot{I}_{np} . We review the somewhat compact derivation of $\frac{\dot{p}}{\delta t}$ in the more general case, specialized for semi-Markov input. This requires finding an expression for

$\Pr(Y_t = y, X_{t+\Delta t} = x)$ as an expansion in Δt . We start as usual:

$$\Pr(Y_t = y, X_{t+\Delta t} = x) = \sum_{x'} \int_0^\infty \Pr(Y_t = y, X_{t+\Delta t} = x, X_t = x', \mathcal{T}_t = \tau) d\tau$$

and utilize the Markov chain $Y_t \rightarrow \mathcal{S}_t^+ \rightarrow X_{t+\Delta t}$, giving:

$$\Pr(Y_t = y, X_{t+\Delta t} = x) = \sum_{x'} \int_0^\infty \Pr(Y_t = y | X_t = x', \mathcal{T}_t = \tau) \Pr(X_{t+\Delta t} = x | X_t = x', \mathcal{T}_t = \tau) \rho(x', \tau) d\tau . \quad (\text{S19})$$

We have $\Pr(Y_t = y | X_t = x, \mathcal{T}_t = \tau)$ from Eq. (S11). So, we turn our attention to finding $\Pr(X_{t+\Delta t} = x | X_t = x', \mathcal{T}_t = \tau)$. Some thought reveals that:

$$\Pr(X_{t+\Delta t} = x | X_t = x', \mathcal{T}_t = \tau) = \begin{cases} q(x|x') \frac{\phi_{x'}(\tau)}{\Phi_{x'}(\tau)} \Delta t & x \neq x' \\ \frac{\Phi_{x'}(\tau + \Delta t)}{\Phi_{x'}(\tau)} & x = x' \end{cases} , \quad (\text{S20})$$

plus corrections of $O(\Delta t^2)$. We substitute Eq. (S20) into Eq. (S19) to get:

$$\begin{aligned} \Pr(Y_t = y, X_{t+\Delta t} = x) &= \left(\sum_{x' \neq x} \int_0^\infty \Pr(Y_t = y | X_t = x', \mathcal{T}_t = \tau) q(x|x') \frac{\phi_{x'}(\tau)}{\Phi_{x'}(\tau)} \rho(x', \tau) d\tau \right) \Delta t \\ &\quad + \int_0^\infty \Pr(Y_t = y | X_t = x, \mathcal{T}_t = \tau) \frac{\Phi_x(\tau + \Delta t)}{\Phi_x(\tau)} \rho(x, \tau) d\tau , \end{aligned}$$

plus corrections of $O(\Delta t^2)$. Recalling:

$$\frac{\Phi_x(\tau + \Delta t)}{\Phi_x(\tau)} = 1 - \frac{\phi_x(\tau)}{\Phi_x(\tau)} \Delta t ,$$

plus corrections of $O(\Delta t^2)$, we simplify further:

$$\begin{aligned} \Pr(Y_t = y, X_{t+\Delta t} = x) &= \left(\sum_{x' \neq x} \int_0^\infty \Pr(Y_t = y | X_t = x', \mathcal{T}_t = \tau) q(x|x') \frac{\phi_{x'}(\tau)}{\Phi_{x'}(\tau)} \rho(x', \tau) d\tau \right) \Delta t \\ &\quad + \int_0^\infty \Pr(Y_t = y | X_t = x, \mathcal{T}_t = \tau) \rho(x, \tau) d\tau \\ &\quad - \left(\int_0^\infty \Pr(Y_t = y | X_t = x, \mathcal{T}_t = \tau) \frac{\phi_x(\tau)}{\Phi_x(\tau)} \rho(x, \tau) d\tau \right) \Delta t , \end{aligned}$$

plus $O(\Delta t^2)$ corrections. We notice that:

$$\int_0^\infty \Pr(Y_t = y | X_t = x, \mathcal{T}_t = \tau) \rho(x, \tau) d\tau = \Pr(Y_t = y, X_t = x) ,$$

so that:

$$\begin{aligned} \lim_{\Delta t \rightarrow 0} \frac{\Pr(Y_t = y, X_{t+\Delta t} = x) - \Pr(Y_t = y, X_t = x)}{\Delta t} &= \sum_{x' \neq x} \int_0^\infty \Pr(Y_t = y | X_t = x', \mathcal{T}_t = \tau) q(x|x') \frac{\phi_{x'}(\tau)}{\Phi_{x'}(\tau)} \rho(x', \tau) d\tau \\ &\quad - \int_0^\infty \Pr(Y_t = y | X_t = x, \mathcal{T}_t = \tau) \frac{\phi_x(\tau)}{\Phi_x(\tau)} \rho(x, \tau) d\tau . \end{aligned}$$

Substituting Eqs. (S11) and (1) into the above expressions yields:

$$\sum_{x' \neq x} \int_0^\infty \Pr(Y_t = y | X_t = x', \mathcal{T}_t = \tau) q(x|x') \frac{\phi_{x'}(\tau)}{\Phi_{x'}(\tau)} \rho(x', \tau) d\tau = \sum_{x'} q(x|x') \left(\left(\int_0^\infty \phi_{x'}(\tau) e^{M(x')\tau} d\tau \right) \bar{u}(x') \right)_y$$

and:

$$\int_0^\infty \Pr(Y_t = y | X_t = x, \mathcal{T}_t = \tau) \frac{\phi_x(\tau)}{\Phi_x(\tau)} \rho(x, \tau) d\tau = \left(\left(\int_0^\infty \phi_x(\tau) e^{M(x)\tau} d\tau \right) \bar{u}(x) \right)_y,$$

so that we have:

$$\begin{aligned} \lim_{\Delta t \rightarrow 0} \frac{\Pr(Y_t = y, X_{t+\Delta t} = x) - \Pr(Y_t = y, X_t = x)}{\Delta t} \\ = \left(\sum_{x'} q(x|x') \left(\int_0^\infty \phi_{x'}(\tau) e^{M(x')\tau} d\tau \right) \bar{u}(x') - \left(\int_0^\infty \phi_x(\tau) e^{M(x)\tau} d\tau \right) \bar{u}(x) \right)_y. \end{aligned}$$

For notational ease, denote the lefthand side as $\delta p(x, y)/\delta t$. The nonpredictive information rate is given by:

$$\begin{aligned} \dot{I}_{\text{np}} &= \lim_{\Delta t \rightarrow 0} \frac{I[X_t; Y_t] - I[X_{t+\Delta t}; Y_t]}{\Delta t} \\ &= \lim_{\Delta t \rightarrow 0} \frac{(H[X_t] + H[Y_t] - H[X_t, Y_t]) - (H[X_{t+\Delta t}] + H[Y_t] - H[X_{t+\Delta t}, Y_t])}{\Delta t} \\ &= \lim_{\Delta t \rightarrow 0} \frac{H[X_{t+\Delta t}, Y_t] - H[X_t, Y_t]}{\Delta t}, \end{aligned}$$

where we utilize stationarity to assert $H[X_t] = H[X_{t+\Delta t}]$. Then, correct to $O(\Delta t)$, we have:

$$\begin{aligned} H[X_{t+\Delta t}, Y_t] &= - \sum_{x,y} \left(p(x, y) + \frac{\delta p(x, y)}{\delta t} \Delta t \right) \log \left(p(x, y) + \frac{\delta p(x, y)}{\delta t} \Delta t \right) \\ &= - \sum_{x,y} p(x, y) \log p(x, y) - \sum_{x,y} p(x, y) \frac{\delta p(x, y)/\delta t}{p(x, y)} \Delta t - \sum_{x,y} \frac{\delta p(x, y)}{\delta t} \log p(x, y) \Delta t \\ &= H[X_t; Y_t] - \sum_{x,y} \frac{\delta p(x, y)}{\delta t} \log p(x, y) \Delta t, \end{aligned}$$

which implies:

$$\dot{I}_{\text{np}} = \sum_{x,y} \frac{\delta p(x, y)}{\delta t} \log p(x, y),$$

with:

$$\frac{\delta p(x, y)}{\delta t} = \left(\sum_{x'} q(x|x') \left(\int_0^\infty \Phi_{x'}(\tau) e^{M(x')\tau} d\tau \right) \bar{u}(x') - \left(\int_0^\infty \phi_x(\tau) e^{M(x)\tau} d\tau \right) \bar{u}(x) \right)_y \quad (\text{S21})$$

and $p(x, y)$ given in Eq. (S18).
